Influence of Ionic Strength on the Actomyosin Reaction Steps in Contracting Skeletal Muscle Fibers

Hiroyuki Iwamoto

Department of Physiology, School of Medicine, Teikyo University, Tokyo, and Experimental Research Division, SPring-8, JASRI, Hyogo 679-5198, Japan

ABSTRACT   Muscle contraction occurs as the result of actin-myosin interaction, which is mediated by the intermolecular forces exerted at the actin-myosin interface. To obtain information about the nature of these intermolecular forces, we tested the sensitivity of various contractile parameters of skinned skeletal muscle fibers to ionic strength (IS) at 3–5°C; IS variation is a useful technique for distinguishing between ionic and nonionic (primarily hydrophobic) types of intermolecular forces. The most striking effect of elevated IS was the strong suppression of isometric tension. However, none of the measured parameters suggested a corresponding decrease in the number of force-generating myosin heads on actin. The rate of actin-myosin association seemed to be only modestly IS-sensitive. The following force-generating isomerization was apparently IS-insensitive. The dissociation of the force-generating actomyosin complex was decelerated by elevated IS, contrary to the expectation from the suppressed isometric tension. These results led us to conclude that an IS-sensitive step, responsible for the large suppression of tension, occurs after force-generating isomerization but before dissociation. The present study suggests that the actomyosin interaction is generally nonionic in nature, but there are at least two ionic processes, one at the beginning and the other close to the end of the actomyosin interaction.

INTRODUCTION

Recently solved atomic structure of the subfragment-1 (S1) of skeletal muscle myosin (Rayment et al., 1993b) revealed that an S1 consists of two major domains: the motor domain, which contains the nucleotide- and actin-binding sites, and the long α-helical light chain-binding domain. Using isolated S1 or its truncated forms, a number of studies have shown evidence that the light chain-binding domain swings on the motor domain in a nucleotide-dependent manner (Fisher et al., 1995; Suzuki et al., 1998; Wakabayashi et al., 1992; Xiao et al., 1998). The fluorescent probe studies have shown that this swing also occurs in contracting muscle fibers (Baker et al., 1998; Hopkins et al., 1998; Irving et al., 1995), and some x-ray diffraction studies support this view (Dobbie et al., 1998). These studies have led to a picture that the contractile force is generated by the nucleotide-driven swing of the light chain-binding domain on the motor domain, which is attached to actin in a rather stationary manner.

In contrast, relatively little attention has been paid to the events taking place at the actin-myosin interface. These events should be as important as the structural changes in myosin within itself. First of all, the Mg-ATPase activity of myosin is activated by actin by orders of magnitude. The force generated by myosin is transmitted to actin via the interface. The mechanical conditions under which muscle fibers are placed, such as shortening, stretching, or quick length steps, are transmitted from actin to myosin via the interface and profoundly influence the performance of myosin. It is clear from these considerations that the actin-myosin interface and the intermolecular forces involved in it play more important, dynamic roles than simply holding actin and myosin together.

In fact, there is biochemical evidence that different parts of the interface are implicated in different stages of actomyosin cycle (Mejean et al., 1986; DasGupta and Reisler, 1989; Brenner et al., 1991). In particular, it is postulated from the crystal structure of S1 that the early, nonstereospecific ionic interaction between the negatively charged N terminus of actin and the positively charged loop of myosin is replaced by stereospecific, hydrophobic interactions in rigor (Rayment et al., 1993a). Thermodynamic studies support this idea (Highsmith and Murphy, 1992; Murphy et al., 1996; Zhao and Kawai, 1994). For the understanding of the entire mechanism of contraction, however, systematic studies must be carried out to clarify the nature and role of the intermolecular forces in each step of actomyosin reaction.

Using skinned skeletal muscle fibers, we approached this issue by examining the effect of ionic strength (IS) on various contractile parameters, which reflect various steps of actomyosin reaction. We tried to cover as many key reaction steps as possible. We adopted the technique of IS variation because of its ability to distinguish between ionic and nonionic forms of intermolecular interactions. (The ionic interaction refers to the association of proteins mediated by electrostatic attraction in aqueous environment, and the nonionic interaction refers to that mediated by hydrophobic attraction. In the latter case, the protein interaction is often strengthened by stereospecific short-range forces that do include some ionic component, but solvent molecules are no longer involved (Ross and Subramanian, 1981).)

The present study is focused on the mechanism responsible for the large effect of IS on isometric tension. To elucidate this, we first test the IS sensitivity of the association/dissociation rate constants of actomyosin in terms of a two-state model (Huxley, 1957). After showing that these parameters do not fully account for the IS effect on tension, we test the IS sensitivity of actomyosin complex formed after association but before force-generating isomerization (specifically, the low-force actomyosin complex; Iwamoto, 1995a). This complex seems to be IS-insensitive. From these results we conclude that some IS-sensitive process must reside in the force-generating actomyosin complex itself. Finally we show in a model calculation that incorporation of a set of force-generating substates, the equilibrium between which is IS-sensitive, would explain the present and previously published results.

The present results revealed a complex interplay of ionic and nonionic interactions throughout the course of contraction. Roles of various intermolecular forces in the actomyosin complex are discussed in light of published knowledge about protein interactions in general. Preliminary results of this study have appeared elsewhere (Iwamoto, 1998a).

MATERIALS AND METHODS

Fiber preparations

Skinned muscle fibers (single fibers or thin bundles of two or three fibers) were isolated from thicker rabbit psoas fiber bundles that had been treated with 0.5% Triton X-100 and stored in a 50% mixture of glycerol and relaxing solution (Iwamoto, 1995a). The fibers were mounted on the experimental apparatus equipped with a force transducer (AE801; Senso-Nor, Horten, Norway) and a servo motor (G120D; General Scanning, Waterton, MA). Sarcomere lengths were adjusted to 2.5 μm by He-Ne laser diffraction.

Experiments on fibers activated by solution exchange

The solutions were basically the same as those of Iwamoto (1998b): the standard relaxing solution contained 80 mM K-propionate, 20 mM imidazole, 10 mM EGTA, 4 mM ATP, 5 mM MgCl$_2$, 20 mM phosphocreatine (Sigma, St. Louis, MO), 125 U/ml creatine phosphokinase (Sigma), and 4% (w/v) dextran T-500 (Pharmacia, Uppsala, Sweden) (pH 7.2, IS = 200 mM). The preactivating solution contained 0.1 mM EGTA, and the contracting solution contained 10.1 mM CaCl$_2$, in addition to the components of the relaxing solution. The IS was adjusted by varying K-propionate concentrations. Different values of IS were used in a random sequence, and at the end of each experiment, contractions were repeated at the initial IS value. Good recovery (nearly 100%) of isometric tension was obtained, even after contractions at IS = 520 mM, indicating that K-propionate does not dissolve myosin filaments at this IS (see also Andrews et al., 1991). In the experiments that studied the effect of inorganic phosphate (P$_i$), 20 mM P$_i$ was included in all three solutions.

The contraction-relaxation cycles were repeated according to the protocol described (Iwamoto, 1995a). The digital servo-control circuits for isotonic release and ramp- or step-length change experiments were basically the same as those described (Iwamoto, 1995b, 1998b). The rate of tension redevelopment after shortening was determined in two protocols. In one, the fibers were made to shorten under a constant load of 0.05P_o (isometric tension) for 60 ms. In this case, the distance of shortening

depended on the shortening velocity, which tended to be smaller at higher values of IS. In the other protocol, the fibers were subjected to unloaded shortening with a large quick release (4% of fiber length). In this case, the distance of shortening was constant, and the time of the onset of tension redevelopment varied depending on velocity. To avoid possible effects of stretch on the rate of rise, the fibers were not stretched back to their original length at the end of shortening in any of these protocols. The command for sinusoidal vibrations to measure fiber stiffness was supplied from an arbitrary waveform generator (HP 33120A; Hewlett Packard, Palo Alto, CA). The length and tension signals were digitized and transferred to a 486- or Pentium-based computer for further analysis. All experiments were carried out at 3–5°C.

Experiments on rigor fibers

The rigor solutions lacked ATP, the ATP-regenerating system, and divalent cations, but contained 5 mM EDTA and 5 mM EGTA. Other components were the same as in the relaxing solution (see above). The ADP solution contained 1 mM ADP, 2 mM MgCl$_2$, 225 μM diadenosine pentaphosphate (Sigma), 1 mM glucose, and 40 U/ml hexokinase (Sigma).

To establish the rigor condition, the fibers were transferred from the relaxing solution to the rigor solution containing 20 mM butanedione monoxime (BDM) (Sigma). In this procedure, the rigor condition was established without rigor tension development or sarcomeric disorder (Higuchi et al., 1995). The following experiments were carried out in the absence of BDM.

The stiffness of the rigor fibers was measured by a series of step length increases (Somasundaram et al., 1989). The command for these steps was supplied from the arbitrary waveform generator (HP 33120A).

Caged calcium experiments

The caged Ca^{2+} solution contained 1.5 mM CaCl$_2$, 2 mM nitrophenyl EGTA (Molecular Probes, Eugene, OR), and 10 mM glutathione and lacked EGTA. Other components were the same as in the relaxing solution. The relaxing and preactivating solutions were identical to those described above. After placing the fibers in the preactivating solution for 2 min, the fibers were equilibrated in the caged Ca^{2+} solution in a photolysis chamber (volume, 10 μl) for an additional 2 min before the photolysis. The photolysis was carried out using a Nd-YAG pulse laser (DCR-3; Spectra-Physics, Mountain View, CA) at λ = 355 nm. The laser beams were line-focused onto the fiber with a cylindrical convex lens. Other equipment used was the same as that for solution exchange experiments. Unless otherwise stated, the fibers were activated with saturating [Ca^{2+}], as judged from the comparison with tension at known [Ca^{2+}]. Experiments were done at 3–5°C. The rise of tension after flash (and after shortening of fibers activated by solution exchange) was fitted to a double-exponential association process (Iwamoto, 1998b). The rate constant for the faster component (k_{dev}) is regarded as physiologically relevant (Szczesna et al., 1996; Wahr and Rall, 1997).

Statistical analysis

Data are expressed as mean $\pm$ SD. The difference between experimental and control values were subjected to a paired t-test. p values less than 0.05 were considered significant.

RESULTS

Isometric tension, the rate constant for the rise of tension, fiber stiffness, and velocity of shortening

The first event of actomyosin interaction is the productive encounter between actin and myosin, which creates a pre-

cursor for all of the following reaction intermediates. This process is generally believed to be an ionic process, mediated by the negatively charged N terminus of actin and the positively charged loop of myosin. Because the ions in solution reduce the attraction between charged groups, elevating IS is expected to adversely affect the encounter, reducing the rate of tension generation and the amount of isometric tension. To examine how the contractile parameters are affected by IS, the IS values of the bathing solutions were varied between 120 and 520 mM. The fibers were activated either by caged Ca^{2+} photolysis (Fig. 1) or by conventional solution exchange (Fig. 2). Static and dynamic parameters are also summarized in Figs. 1 and 2.

In agreement with the expectation that elevating IS adversely affects the actin-myosin encounter, the isometric tension was strongly suppressed at high IS values (Figs. 1 and 2). At IS = 520 mM, the isometric tension was 27% and
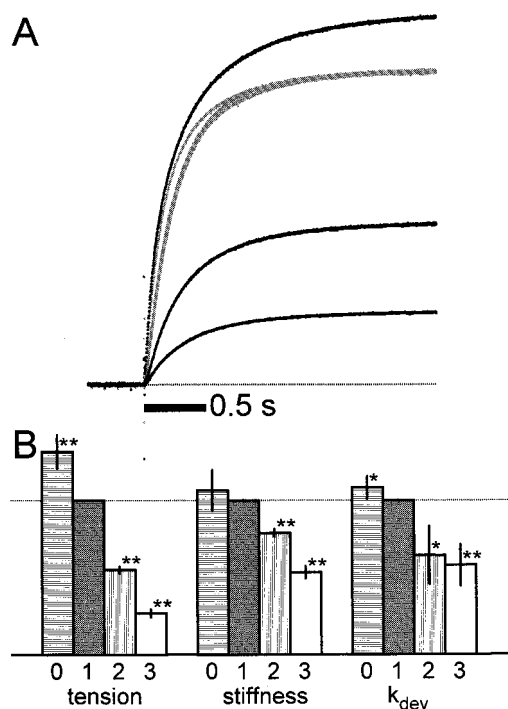

FIGURE 1   Effect of ionic strength (IS) on the contraction of skinned rabbit psoas fibers activated by the photolysis of caged Ca^{2+}. (*A*) time course of rise of isometric tension after photolysis. All records were normalized to the final level of tension reached after photolysis at normal IS (IS = 200 mM, *gray line*; three traces are superimposed). The black traces were obtained at IS values of 120, 360, and 520 mM from above. Three sets of paired records (at normal and high or low IS values) from three different specimens are shown. (*B*) Summary of effects of ionic strength on isometric tension, stiffness, and the rate constant for the rise of tension (k_{dev}) of the fibers activated by caged Ca^{2+} photolysis. All of the values were normalized to the values at normal IS (IS = 200 mM). The columns denoted by 0, 1, 2, and 3 represent the IS values of 120, 200, 360, and 520 mM, respectively. Mean $\pm$ SD ($n = 4–6$). Asterisks mark levels of statistical significance of the difference from control values: *$p < 0.05$; **$p < 0.01$. The absolute value of k_{dev} at IS = 200 mM is 7.2 s^{-1}.
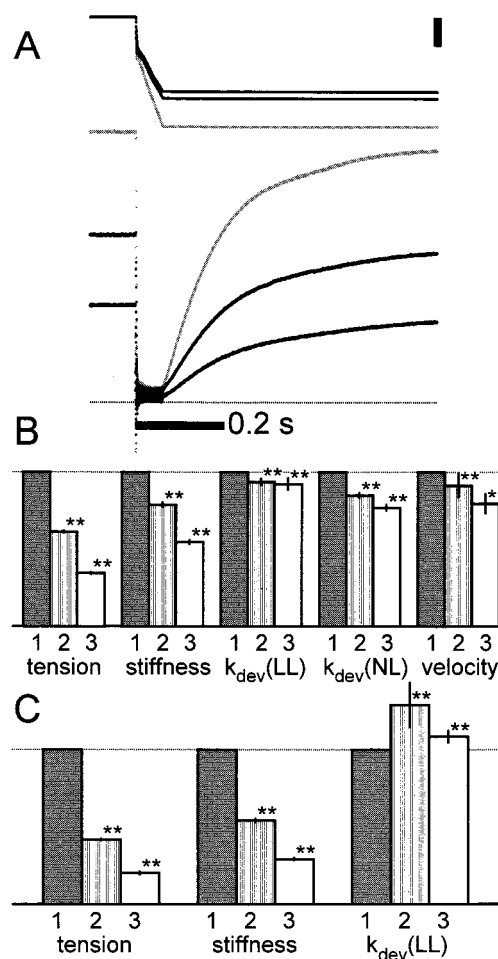

FIGURE 2   Effect of IS on the contraction of skinned rabbit psoas fibers activated by solution exchange. (*A*) Lightly loaded shortening and subsequent redevelopment of isometric tension. The traces above are length records (*scale bar*, 0.5% fiber length). The fibers were made to shorten under a constant load of 5% isometric tension for 60 ms and then were held isometric. Tension records were normalized to the level of tension immediately before shortening at normal IS (IS = 200 mM). Gray lines, records obtained at normal IS; black lines, records for higher IS values. In tension records, the traces are on the order of 360 and 520 mM from above. In length records, the traces are on the order of 360 and 520 mM from below. All traces were recorded from the same specimen. (*B* and *C*) Summary of effects of ionic strength on the static and dynamic parameters of fibers activated by solution exchange. (*B*) From the left, prerelease levels of isometric tension and stiffness, k_{dev}, recorded after lightly loaded shortening (LL, records shown in *A*) and after no-load shortening (NL) (the rate of rise of tension was measured after the fiber was made slack by imposing a large quick release; records not shown) and the velocity of lightly loaded shortening (records shown in *A*). (*C*) Data obtained in the presence of 20 mM P_i. From the left, prerelease levels of isometric tension and stiffness, and k_{dev} recorded after lightly loaded shortening (LL) (records not shown). All of the values were normalized to the values at normal IS (IS = 200 mM). The columns denoted by 1, 2, and 3 represent the IS values of 200, 360, and 520 mM, respectively. Mean $\pm$ SD ($n = 5–8$). Asterisks mark levels of statistical significance of the difference from control values: *$p < 0.05$; **$p < 0.01$. The absolute values of k_{dev} at IS = 200 mM are 8.3 and 14.2 s^{-1}, respectively, in the absence and presence of 20 mM P_i. The shortening velocity in the absence of P_i is 0.33 $\times$ fiber·s^{-1}.

35% of that of control (IS = 200 mM) for fibers activated by caged Ca^{2+} photolysis and solution exchange, respectively.

The rate of initial actin-myosin encounter can directly affect the number of force-generating cross-bridges if the encounter limits the rate of tension development, i.e., the rate constant for the force-generating isomerization is greater than that of the encounter. In this situation, the whole actomyosin reaction cycle can be simplified to a two-state scheme, ruled by the association (*f*) and dissociation (*g*) rate constants (Huxley, 1957). (In the absence of P_i, *f* and *g* roughly correspond to k_{+2} and k_{+6} in the scheme in Fig. 8.) Here, the rate constant for the rise of tension (k_{dev}) is the sum of *f* and *g*. Therefore, if the reduced rate of actin-myosin encounter (i.e., *f*) is fully responsible for the large decrease in isometric tension, k_{dev} should exhibit a similar sensitivity to IS unless *g* is unrealistically large (see the Discussion for a more quantitative account).

Although the results showed that k_{dev} was sensitive to IS, its IS sensitivity was much smaller than that of isometric tension (Fig. 1 *B*). The values of k_{dev} at IS = 520 mM was 58% of control (versus 27% for tension). The IS sensitivity of k_{dev} was even smaller after shortening (Fig. 2 *B*). At 520 mM, k_{dev} was 92% of control after shortening under a constant load of $0.05 \times P_o$ and 77% of control after unloaded shortening (Fig. 2 *B*). These values of IS sensitivity of k_{dev} are too small if the IS sensitivity of *f* is responsible for the strong suppression of isometric tension. (The relatively IS-insensitive k_{dev} may be alternatively due to the IS-dependent increase of *g*. As will be shown below, however, several lines of evidence suggest that this is unlikely.) It is therefore concluded that the rate constant for the initial complex formation is not sensitive enough to explain the large IS sensitivity of tension, and the amount of actomyosin complex formed at high IS should be greater than expected from the amount of tension generated.

In support of this idea, the fiber stiffness (an index for the number of myosin heads attached to actin) was also less sensitive to IS than the isometric tension (Figs. 1 *B* and 2 *B*; Seow and Ford, 1993). The stiffness at IS = 520 mM was 55% of control (versus 35% for tension). The stiffness at high IS values was greater than that of submaximally activated fibers generating a comparable amount of tension at normal IS (Fig. 3). This means that the difference in the IS sensitivity between tension and stiffness is not due entirely to the compliance outside the cross-bridges (see Goldman and Huxley, 1994), but reflects the real reduction of the averaged force per cross-bridge.

The velocity of lightly loaded shortening, which is considered to reflect the rate of actomyosin dissociation, is summarized in the rightmost set of columns in Fig. 2 *B*. The velocity tended to decrease at high IS values (~20% decrease at IS = 520 mM), although previous studies report little effect (Gulati and Podolsky, 1981; Julian and Moss, 1981; Seow and Ford, 1993). The result is not in favor of the
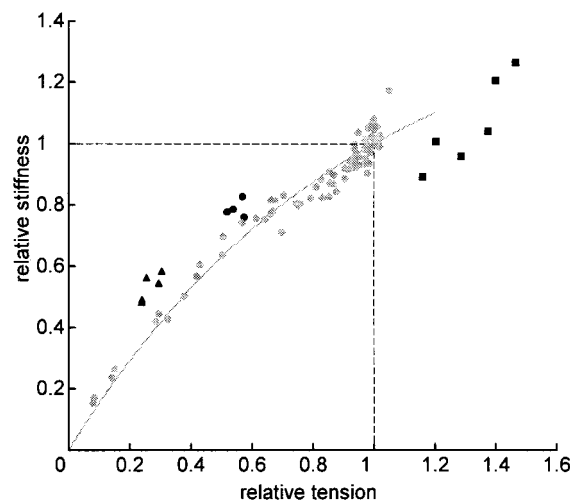

FIGURE 3 The relation between isometric tension and stiffness of fibers activated by caged Ca^{2+} photolysis. The values were normalized to those of fibers fully activated at IS = 200 mM. Black squares, fully activated at IS = 120 mM; black circles, fully activated at IS = 360 mM; black triangles, fully activated at IS = 520 mM; gray circles, activated to various levels at normal IS (200 mM) by reduction of the energy of the laser flash. The line (single exponential association) is drawn only to assist the eye.

idea that the actomyosin dissociation (*g*) is accelerated by increased IS.

The effects of IS on tension, stiffness, and k_{dev} were also determined in the presence of 20 mM P_i (Fig. 2 *C*). The sensitivity of tension or stiffness to IS was increased by the addition of P_i (for tension, 20% versus 35% of control at $I = 520$ mM). The IS-dependent decrease in k_{dev} is no longer obvious, as expected from the contribution of the P_i-induced reversal of the force-generating isomerization to k_{dev}.

To summarize, the reduced interaction between the charged groups of actin and myosin at elevated IS accounts for only a part of the large suppression of isometric tension. Therefore a step (steps) later than the initial encounter should be responsible for the rest of the IS-induced tension suppression.

Kinetics of low-force actomyosin complex

After the initial encounter between actin and myosin, evidence is accumulating that a low-force actomyosin complex is formed before the force-generating complex. The low-force complex contributes to fiber stiffness (Brozovich et al., 1988; Iwamoto, 1995; Regnier et al., 1995) and has slow dissociation kinetics (Iwamoto, 1995a), and its population is increased in the presence of P_i (Brozovich et al., 1988; Iwamoto, 1995a) during shortening (Iwamoto, 1995b) and probably during the rise of tension (Iwamoto et al., 1995).

The transition from the low-force to force-generating complexes (force-generating isomerization) is a good candidate for the step to be inhibited by elevated IS. If this is

the case, elevated IS should cause the accumulation of the actomyosin in the form of low-force complex. We attempted to determine whether elevated IS increases the population of the low-force complex.

Our protocol for detecting the low-force complex utilizes its unique nonlinear response to stretch: when the low-force complex is strained more than ~4 nm (~0.3% of fiber length), its stiffness suddenly increases (Iwamoto, 1995a,b). As a result, the stretch amplitude-response curve shows a characteristic flection at ~0.3% of fiber length.

Fig. 4 shows the records of an experiment in which fibers were stretched by various amplitudes at the isometric plateau at IS = 360 mM, in either the presence or absence of 20 mM P_i. In the absence of P_i, the magnitude of the tension response was almost proportional to the stretch amplitude, showing little sign of increased low-force cross-bridge population (Fig. 4 A). On the other hand, the addition of 20 mM P_i made the tension response highly nonlinear (Fig. 4 B),
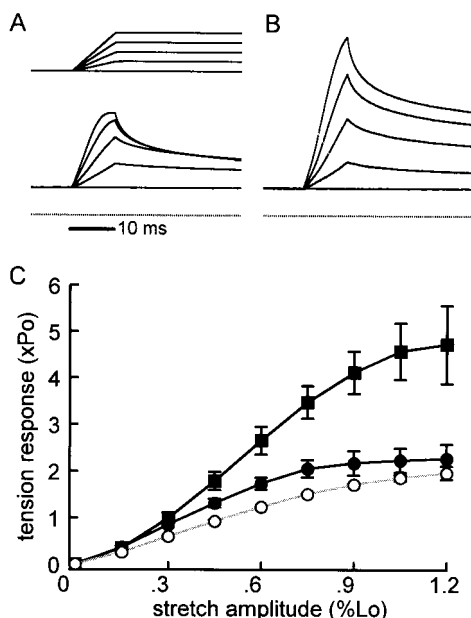

FIGURE 4 Tension responses to ramp stretches of various amplitudes (duration, 10 ms; amplitude, 0.3–1.2% fiber length in 0.3% steps) recorded at the plateau of contraction initiated by solution exchange. (A and B) Traces of tension (*below*) and length (*above*) recorded at an isometric plateau at IS = 360 mM in the absence (A) and presence (B) of 20 mM P_i. Four traces are superposed. Tension records were normalized to the prestretch level (P_o). The dotted line represents the zero-tension level. Note that the tension responses to a 0.3% stretch are not different, but for larger stretches the tension responses become disproportionately greater in the presence of P_i (B). (C) The relation between stretch amplitude and the magnitude of tension response, defined as the difference between the prerelease level of tension and the peak tension attained at the point where the stretch stopped. ○, IS = 200 mM, − P_i; ●, IS = 360 mM, − P_i; ■, IS = 360 mM, + 20 mM P_i. Note the increased slope of the curve in the presence of P_i at stretch amplitudes of ~0.3% fiber length (L_o) and greater. Mean ± SD (n = 6, n = 2 for IS = 200 mM). For more results for IS = 200 mM see Iwamoto (1995a,b).

indicating that the low-force cross-bridge population was increased just as in normal IS (Iwamoto, 1995a,b). This situation is clear in the stretch amplitude-response curves, as shown in Fig. 4 C, in which the characteristic flexion of the curve is observed only in the presence of 20 mM P_i.

The population of the low-force cross-bridges is also expected to increase during the rise of tension after calcium activation (see Iwamoto et al., 1995). The stretch amplitude-response curves were also obtained during the rise of tension after caged Ca^{2+} photolysis (stretched 150 ms after flash, when ~30% of the steady-state force had developed) at normal and high IS values. As in the presence of P_i, the response to stretch was nonlinear regardless of IS (Fig. 5, A and C), indicating that the low-force cross-bridges are equally well populated at both IS values. The stretch amplitude-response curves have a flexion at ~0.3%, and the curves for the two IS values are superimposable (Fig. 5 E). When the fibers were stretched at the plateau (stretched 3 s after flash), most of the nonlinearity had disappeared regardless of IS (Fig. 5, B and D), and again the curves for the two IS values are superimposable (Fig. 5 F).

To summarize, the population of the low-force cross-bridges responded to experimental perturbations in a uniform manner regardless of IS. The results therefore suggest that the force-generating isomerization and its P_i-induced reversal are unaffected by elevated IS.

Kinetics of force-generating cross-bridges

It is known that the ATPase activity of the fiber is suppressed less than isometric tension at elevated IS (Kawai et al., 1990; Godt et al., 1993). In the model in which a single turnover of ATPase reaction is tightly coupled to a cross-bridge dissociation from actin (Huxley, 1957), the relative insensitivity of the fiber ATPase activity would be explained if the dissociation rate constant were to increase at high IS values. This would also partly explain the relative insensitivity of k_{dev} to IS, because k_{dev} is the sum of the association (*f*) and dissociation (*g*) rate constants in terms of Huxley's (1957) two-state model. However, we have shown that this possibility is not supported by the observation that elevated IS failed to increase the shortening velocity (Fig. 2). Here we show more direct evidence that the dissociation rate constant is not accelerated by elevated IS.

At physiological ATP concentrations, the rate of the dissociation of force-generating cross-bridges is probably limited by the dissociation of ADP from myosin (Dantzig et al., 1991). Under isometric conditions it is difficult to extract the dissociation rate constant because of its slowness. However, the dissociation rate constant is more easily measured after a quick reduction in length (quick release) because it is expected to be remarkably increased by the release and to become dominant over the association rate constant.
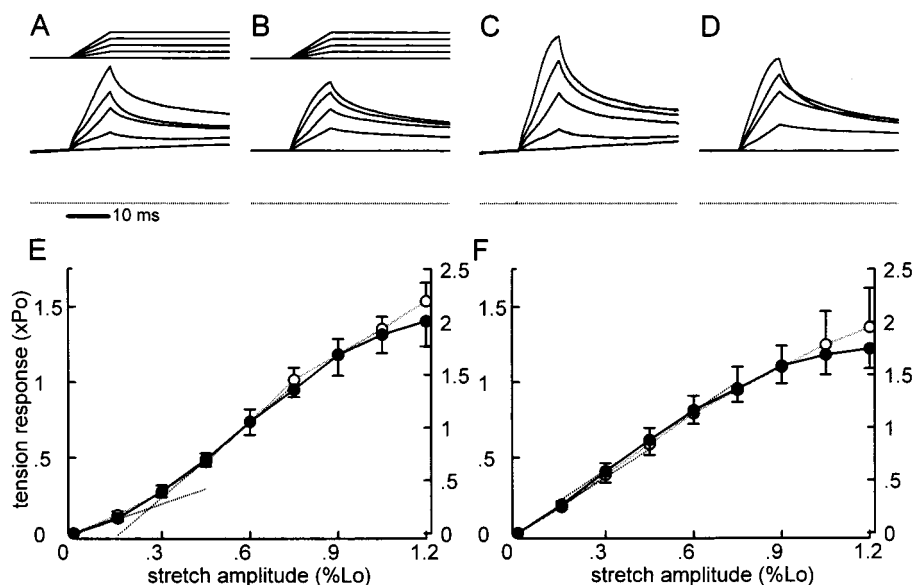
FIGURE 5 Tension responses to ramp stretches of various amplitudes (duration, 10 ms; amplitude, 0.3–1.2% fiber length in 0.3% steps) recorded in the rising phase or at the plateau of contraction initiated by caged Ca^{2+} photolysis. (*A* and *B*) Tension and length traces recorded at IS = 200 mM. (*C* and *D*) Tension traces recorded at IS = 360 mM. Traces were obtained 150 ms (*A* and *C*, rising phase; ~30% of full isometric tension has developed) and 3 s (*B* and *D*, isometric plateau) after flash photolysis of caged Ca^{2+}. The tension traces were normalized to the level immediately before stretch. Note the disproportionately enhanced tension response to stretches greater than 0.3% of fiber length (L_o) in the rising phase at both IS values (*A* and *C*). (*E* and *F*) The relation between stretch amplitude and the magnitude of tension response to stretches applied 150 ms (*E*) and 3 s (*F*) after photolysis. ○, IS = 200 mM; ●, IS = 360 mM. The scale of the ordinate to the left applies to IS = 200 mM; that to the right applies to IS = 360 mM. The line connecting the data points at 0 and 0.15% L_o and the line connecting those at 0.45 and 0.6% L_o are extended with dotted lines to stress the difference in the shape of curves between *E* and *F*. Note that the curves are nonlinear around 0.3% in *E* and more linear in *F*, regardless of IS. Mean ± SD ($n = 6$).

In the experiment shown in Fig. 6, the dissociation rate constant was determined from the rate of decay of stiffness (k_{decay}) after a quick release. After the release (amplitude,

0.8% fiber length; complete in 1 ms), the tension quickly recovered (phase 2 of Huxley and Simmons, 1971) and then stayed constant for a while (phase 3) before the final ap-
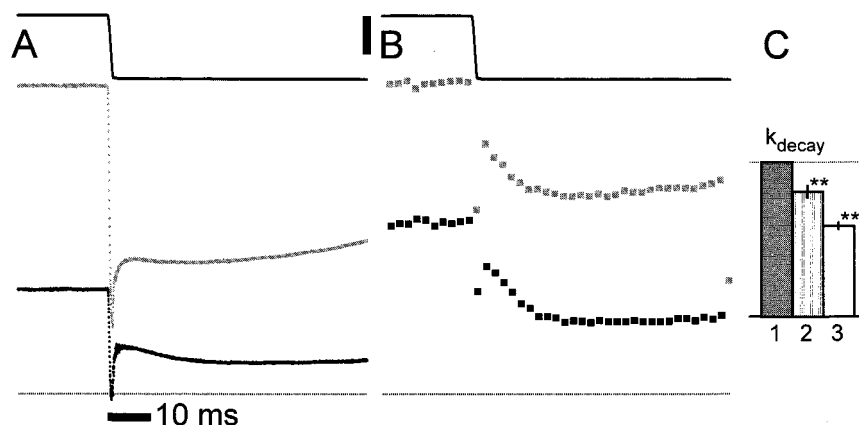

FIGURE 6 Measurement of the rate constant for the decay of stiffness (k_{decay}) after a quick release. Most of the decay occurs during the plateau period (phase 3; see Huxley and Simmons, 1971) of tension transient. (*A*) Tension response to a quick release (0.8% fiber length, complete in 1 ms, *trace above*; *scale bar*, 0.5% fiber length). (*B*) Accompanying changes of stiffness (*squares*) measured with sinusoidal oscillation (0.2% fiber length in peak-to-peak amplitude, 1 kHz). Records were normalized to their prerelease levels at normal IS (*gray line and squares*). Solid records are obtained at 520 mM. Traces were recorded from the same specimen. (*C*) Summary of the IS effect on k_{decay}, normalized to the value at IS = 200 mM. For the meaning of numbers and asterisks by the columns see Fig. 1. Mean ± SD ($n = 6$). The absolute value for k_{decay} at IS = 200 mM is 160 s^{-1}.

proach to the prerelease level of tension. Meanwhile, the fiber stiffness continued to decay in an exponential manner. The fitted rate constant for the stiffness decay (k_{decay}) decreased with increasing IS (59% of control at IS = 520 mM; Fig. 6 C).

In summary, the result did not support the hypothesis that the tension suppression at high IS is due to the accelerated dissociation of the force-generating cross-bridges.

Rigor stiffness

The final stage of actomyosin complex before the ATP-induced dissociation is rigor, although this rigor complex should exist only transiently at physiological ATP concentrations. To determine whether the fiber stiffness is sensitive to IS in rigor, the fiber was subjected to a series of step stretches in a protocol similar to that of Somasundaram et al. (1989) (Fig. 7 A). The fiber stiffness, or the increment of tension at each step, tended to saturate as the total amount of stretch increased, but a complete saturation was not obtained. Therefore the highest values of stiffness obtained were compared for different experimental conditions. The stiffness was remarkably insensitive to IS (Fig. 7 B), and the traces of tension for different IS values were almost perfectly superimposable.

DISCUSSION

Relationship to earlier studies

A large number of papers have been published on the effect of ionic strength (IS) on the properties of muscle fibers or

FIGURE 7 Effect of IS on rigor stiffness. (*A*) Tension response (traces below) of rigor fibers to a series of stretches of equal amplitude (*traces above; scale bar*, 0.5% fiber length). The tension increment with a step (or stiffness (*squares*) in arbitrary units) increased with steps but tended to saturate. The gray and black records are for normal and 520 mM IS, respectively. All data were recorded from the same specimen. (*B*) Summary of the IS effect on rigor stiffness. The highest values of stiffness recorded in a single series of stretches were normalized to those at IS = 200 mM. For the meaning of the numbers and asterisks by the columns, see Fig. 1. Mean ± SD ($n = 6$).

contractile proteins. Many of the studies were conducted in the range of IS lower than the physiological value, where a significant fraction of weakly binding actomyosin complex exists in its attached form (see Brenner, 1987, for a review). In contrast, relatively few papers (including the present paper) put their focus on the range of IS higher than the physiological value.

In physicochemical terms, the action of IS in the low-IS range is distinguished from that in the high IS, as discussed below in detail, and the border may be drawn at 100 mM. At IS values far below 100 mM, long-range interactions between charged molecules would be the major events. In the range above 100 mM, such interactions are no longer possible- and, if significant IS effects are found, different mechanisms must be sought.

A number of papers described the properties of contracting muscle fibers in this high-IS region (Godt et al., 1993; Kawai et al., 1990; Seow and Ford, 1993). All of these studies reported a significant reduction of isometric tension at high IS values. The first two reported that the fiber ATPase activity is relatively insensitive to IS. Both studies reported parallel decreases in tension and stiffness and ascribed the relative insensitivity of ATPase to an increase in the dissociation rate constant. On the other hand, Seow and Ford (1993) reported a higher stiffness/tension ratio at elevated IS values as we report here and ascribed the effect to the detention of the cross-bridges to one of the A·M·ADP·P$_i$ states.

The steps affected by ionic strength in the sequence of actomyosin reaction

In the present study, we examined the effect of elevating IS on the steps of actomyosin reaction, to obtain information about the physicochemical nature of intermolecular contacts made in the process of muscle contraction. We followed the sequence of reaction steps in the ATPase cycle, starting with the initial encounter between actin and myosin.

The first encounter generates the collision complex of actin and myosin. The step immediately after this is likely to be a first-order reaction with respect to the concentration of the collision complex, which is determined by the affinity of myosin for actin. This step is in turn expected to affect the rate of later reaction steps for tension development. Present results showed that IS variation has only a modest effect on the rate constant for tension development (k_{dev}), while it has a profound effect on isometric tension.

In terms of a two-state model (Huxley, 1957), the only explanation for the much smaller IS sensitivity of k_{dev} than that of tension is that the dissociation rate constant (g) is comparable to or greater than the association rate constant (f). This implies that only a small fraction of myosin heads are attached to actin at a time, and that the ATPase activity is relatively high. For the rise of tension after unloaded shortening, for example, the expected ratio of f: g at normal
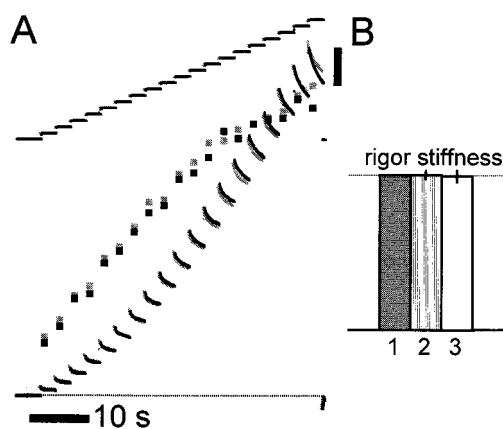
IS is ~3:7 (i.e., only 30% of total myosin is attached to actin), and ATPase is ~1.9 s^{-1}. (In the two-state model, the tension is proportional to $f/(f + g)$, and the ATPase rate is $fg/(f + g)$. The k_{dev} is expressed as $f + g$ and was 9.16 s^{-1} in this particular experiment.) However, the measured ATPase activity of fiber at normal IS is ~1.1 s^{-1} at 10°C (Iwamoto, 1998c) and should be lower at the temperature we used here. From these considerations, it is clear that the large IS sensitivity of isometric tension is not explained by the IS dependence of the rate of the initial encounter alone.

Next we attempted to determine whether the IS sensitivity of the force-generating isomerization is responsible for the large suppression of isometric tension. However, this possibility was eliminated by the observation that the population of the low-force complex is hardly affected by IS variation (Figs. 4 and 5). Therefore, the IS-dependent step should come after the force-generating isomerization. Because of its remarkable insensitivity to IS, the low-force actomyosin complex is clearly distinguished from the weakly binding complex. Seow and Ford (1993) postulated that the elevated IS detains the actomyosin complex in a low-force form. This form is clearly distinct from the low-force complex referred to in this paper, because the characteristic nonlinearity is not observed in the tension response to stretch.

After a period of force generation, the actomyosin complex will eventually dissociate. The results showed that the rate constant for the dissociation, at least after a quick release, is decreased by increasing IS (Fig. 6). This is contrary to the expectation from the lowered isometric tension and relatively IS-insensitive fiber MgATPase activity (Kawai et al., 1990; Godt et al., 1993). As it is postulated that the rate of cross-bridge dissociation is limited by the

release of ADP (Dantzig et al., 1991), this result may be taken to mean that the ADP release step is inhibited, not accelerated, by elevated IS. Alternatively, the force-generating cross-bridges may consist of two species (see below), and the species dominant in high IS values may dissociate more slowly than the other. Whichever is the case, the slowed dissociation of cross-bridges at high IS values explains the decrease in the velocity of lightly loaded shortening (Fig. 2).

To summarize, the point of tension-suppressing action of elevated IS should lie in the period between the force-generating isomerization and the dissociation.

Mechanism of action of ionic strength

The question arises whether the IS effect of decreasing isometric tension is kinetic (i.e., IS affects the rate constant(s) in the actomyosin reaction cycle) in nature, or it is simply to reduce the tension per cross-bridge without affecting its kinetics. At least the observation that the elevated IS increases the sensitivity of tension to P_i (Fig. 1 *C*) supports the idea that the IS effect is kinetic (see below).

The simplest explanation for the IS effect to be kinetic would be that there are two substates of force-generating actomyosin complex, and that the transition between them is sensitive to IS. They generate different amounts of tension, and the one generating the lower force is favored at higher IS values. This feature is incorporated into the proposed scheme of actomyosin reaction (Fig. 8), which is an expansion of the previously published scheme (Iwamoto, 1995b). The two force-generating A·M·ADP substates (A·M·ADP(1) and A·M·ADP(2)) are in rapid equilibrium, and the reverse rate
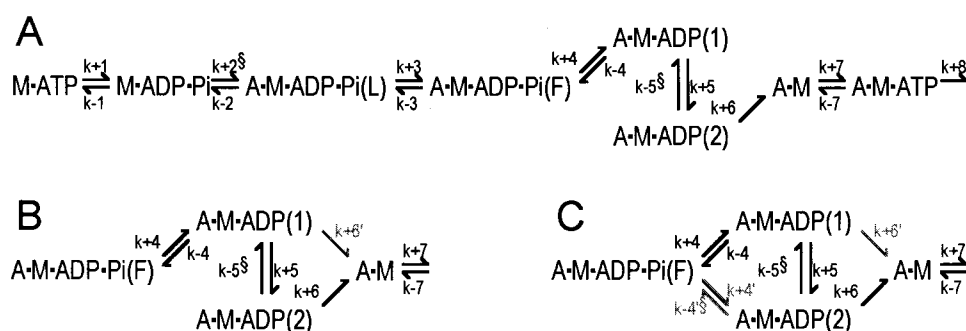

FIGURE 8 Actomyosin reaction scheme proposed to explain the present results. The scheme has three force-generating A·M·ADP substates (denoted by 1 and 2), the latter bearing higher force. Three rate constants (k_{+2}, k_{-4}', and k$_{-5}$, denoted by §) are assumed to be IS-dependent (k_{+2} is decreased, and k_{-4}' and k_{-5} are increased by increasing IS). The release of ADP and the dissociation of A·M·ATP are assumed to be irreversible. Following the low-force A·M·ADP·P$_i$ (denoted by L), a force-generating A·M·ADP·P$_i$ intermediate (denoted by F) is incorporated in the light of a two-step P$_i$ release process (Dantzig et al., 1992; Kawai and Halvorson, 1991). This intermediate, assumed to support the same amount of tension as A·M·ADP (1), does not exist in a significant amount in the absence of P$_i$. (*A*) The whole scheme of ATPase reaction in which all intermediates are aligned in series. The right end of the scheme continues to the left end. (*B*) A part of the scheme in *A*, but with a branch pathway allowing the A·M·ADP(1) to release ADP (*gray arrow and primed rate constant*). (*C*) A part of the scheme in *A*, but with a second branch pathway allowing the direct formation of A·M·ADP(2) from A·M·ADP·P$_i$(F) (*gray arrow* and primed rate constant) along with the branch pathway in *B*.

constant (k_{-5}) is assumed to be IS-sensitive. Fig. 8 shows three possible ways of having these substates in the scheme, and the IS dependence of the contractile parameters was calculated for each case in Fig. 9. In the scheme in Fig. 8 *A*, all of the intermediates are in series. This variation reproduces the increased IS sensitivity of tension in the presence of P_i (Fig. 9, *A* and *B*), but the ATPase activity is also very sensitive to IS. This is clearly at odds with the observation (Godt et al., 1993; Kawai et al., 1990). The variation in Fig. 8 *B* incorporates a branch pathway that allows the lower force A·M·ADP(1) to release ADP and form a rigor complex. In this variation, the P_i-induced sensitization to IS is retained, while the ATPase rate is relatively IS-insensitive (Fig. 9, *C* and *D*). The third variation (Fig. 8 *C*) has a second branch pathway that permits the formation of A·M·ADP(2) from the force-generating A·M·ADP·P_i intermediate. The detailed-balance considerations require that this step also be IS-sensitive. In Fig. 8 *C*, k_{-4}' is assumed to have the same IS sensitivity as k_{-5}. The results of the model calculation for this variation (not shown) were almost identical to those in Fig. 9, *C* and *D*.

Therefore, the present consideration cannot distinguish between the second and third variations. However, the conclusion still holds that both A·M·ADP substates should be able to release ADP.

The difference in the amounts of force supported by the two A·M·ADP substates can be quite large. In fact, the calculation in Fig. 9 assumes that A·M·ADP(1) produces only 20% of force produced by A·M·ADP(2). The difference in this magnitude is needed to reproduce the observed IS sensitivity of tension.

A feature common to the three variations of scheme in Fig. 8 is that the ATPase activity is very sensitive to P_i. However, it has been shown that the ATPase activity is less sensitive to P_i than is tension (Ebus et al., 1994; Kawai et al., 1987). To solve this paradox, one may use a logic similar to that used to explain the relative insensitivity of ATPase activity to IS: one may assume a third branch pathway that allows the force-generating A·M·ADP·P_i complex (A·M·ADP·P_i (F) in Fig. 8; see Dantzig et al., 1992; Kawai and Halvorson, 1991) to release its hydrolysis products all at once. With the set of rate constants given (Fig. 9), this intermediate is significantly populated only in the presence of P_i.

Whether the two proposed A·M·ADP substates correspond to the two configurations assumed in the Huxley and Simmons model (1971) is not clarified in the present study. To test this, one should at least quickly change the IS and measure the rate of the resulting tension transient. The IS effect on tension becomes smaller at higher temperature (data not shown), suggesting that the transition between the two A·M·ADP substates is also sensitive to temperature. There is a suggestion that the tension transient after a temperature jump corresponds to that after a quick release (Davis, 1999). If this is true, it is possible that the two A·M·ADP substates are related to the configurations assumed in the Huxley-Simmons model.
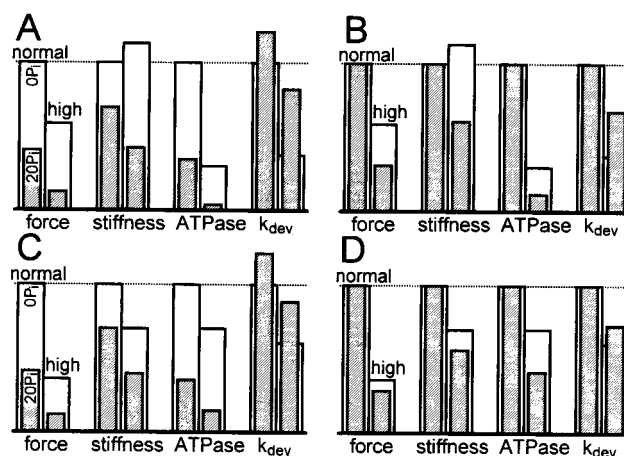

FIGURE 9 Simulated isometric tension, stiffness, ATPase rate, and k_{dev} based on the schemes in Fig. 8. (*A* and *B*) Simulation based on the scheme in Fig. 8 *A*, with all of the intermediates in series. (*C* and *D*) Simulation based on the scheme in Fig. 8 *B*, in which one of the branch pathways (ADP release from A·M·ADP(1)) is allowed. The result of the simulation based on the scheme in Fig. 8 *C*, in which both branch pathways are allowed, is almost identical to that in *C* and *D* and is therefore not shown. In each set of four columns (*two white, two shaded*), the two columns (*one white, one shaded*) on the left side represent the values at normal IS, and the two on the right represent the values at high IS (intended to reproduce the results at 520 mM). The white and hatched columns represent, respectively, values in the absence and presence of 20 mM P_i. In *A* and *C* the values were normalized to the value at normal IS in the absence of P_i. In *B* and *D* the same data as in *A* and *C* were normalized in a different manner to stress the effect of P_i on IS sensitivity: the values were normalized to the value at normal IS at respective concentrations of P_i. The force was calculated by assuming that the force produced by a myosin cross-bridge in the A·M·ADP·P_i(F) or A·M·ADP(1) state is 20% of that produced by a myosin head in the A·M·ADP(2) state. The myosin head in the A·M or A·M·ATP state is assumed to produce the same amount of force and stiffness as that in the A·M·ADP(2) state, although such intermediates are virtually nonexistent with the present set of rate constants. The stiffness was calculated by assuming that all of the force-generating cross-bridges make an equal contribution to the stiffness, while the A·M·ADP·P_i(L) cross-bridges make a 50% contribution. The dissociated forms of intermediates were assumed to bear no stiffness. The time course of rise and the final amount of tension or stiffness were calculated by numerically integrating a set of differential equations derived from the scheme in Fig. 8 and rate constants listed below, with a unit time segment of 40 μs. The initial condition was that all of the intermediates were in the form of M·ADP·P_i. The value of k_{dev} was calculated as the inverse of the time required for the isometric tension to reach its half-maximum. The values of the rate constants used in the simulations are (in s^{-1}) $k_{+1} = 50$; $k_{-1} = 10$; $k_{+2} = 10$ (normal IS) or 3.85 (high IS); $k_{-2} = 10$; $k_{+3} = 100$; $k_{-3} = 200$; $k_{+4} = 2000$; $k_{-4} = 100,000 \times [P_i]$ in M (in *A–D*); $k_{+5} = 100$; $k_{-5} = 100$ (normal IS) or 676 (high IS); $k_{+6} = 6$ (in *A* and *B*) or 3 (in *C* and *D*); $k_{+6}' = 3$; $k_{+7} = 1000$; $k_{-7} = 1000$; $k_{+8} = 1000$. For the calculation for the scheme in Fig. 8 *C* (not shown because the results are almost identical to those in *C* and *D*), the rate constants used are $k_{+4}' = 1000$; $k_{-4}' = 50,000 \times [P_i]$ (normal IS) or 338,000 $\times [P_i]$ (high IS); $k_{+4} = 1000$; $k_{-4} = 50,000 \times [P_i]$. Note the large effect of IS on ATPase in *A* and *B*. The addition of 20 mM P_i increases the sensitivity of tension to IS.

Intermolecular forces

In terms of intermolecular forces, the present results may be summarized as follows: in the actomyosin ATPase pathway, there are at least two ionic processes. One is the initial formation of the actomyosin complex, and the other is a force-augmenting step that comes after the force-generating isomerization. Other processes are generally insensitive to IS and are therefore considered nonionic in nature.

The contribution of ionic force to the initial encounter between actin and myosin is smaller than previously thought, and this is even more true for the tension redevelopment after lightly loaded or unloaded shortening. The long-range electrostatic attraction between protein and freely diffusible charged molecules diminishes as the screening effects of counterions increase. At an IS of 100 mM, the Debye-Hückel theory dictates that the space constant for the decay of electrostatic attraction has fallen to ~ 1 nm (see Cantor and Schimmel, 1980). The hydrophobic attraction has a comparable space constant but decays exponentially over a distance of 10 nm (Israelachvili and Pashley, 1982). At IS values higher than 100 mM, the hydrophobic attraction would be the only long-range force exerted between dissociated protein molecules. The ionic interaction between the N terminus of actin and the lysine-rich loop of myosin, therefore, should play only a limited role in the initial complex formation in this high-IS range. (However, it has been reported that the genetic alteration of the charge of the N terminus of actin or the loop in myosin affects motility in vitro or the ATPase activity (Furch et al., 1998; Sutoh et al., 1991). This may imply that the charged residues at the N terminus may play roles in enzymatic activity in later stages.)

It would be natural to assume that hydrophobic attraction plays a more important role in bringing actin and myosin together at this high IS range. There are several reasons for this: 1) At physiological IS values or higher, actin and myosin are dissociated in the absence of Ca^{2+}, while the N terminus of actin and the lysine-rich loop are exposed to the medium. 2) Upon Ca^{2+} activation, tropomyosin shifts its position to expose the myosin-binding site of actin, which is composed of a cluster of hydrophobic residues (Lehman et al., 1995), and this is complementary to the cluster of hydrophobic residues on myosin (Rayment et al., 1993a). 3) The hydrophobic attraction, an entropic force derived from the destructuring of water, is by nature a long-range force (Israelachvili and Pashley, 1982) that acts rather nonspecifically between hydrophobic surfaces (Chothia and Janin, 1975). Because of this long range of action, the clusters of hydrophobic residues on neighboring actin monomers may be assumed to form a semicontinuous hydrophobic track along which myosin can move while remaining attracted. This may explain why k_{dev} after shortening is even less sensitive to IS than k_{dev} after photolysis of caged Ca^{2+}, and

the intensity ratio of equatorial x-ray reflections (an index for the shift of mass between thick and thin filaments) does not approach its resting value until the shortening velocity is close to V_{max} (Podolsky et al., 1976; Huxley et al., 1988).

The stereospecific interactions between protein surfaces involve short-range forces such as van der Waals contacts and hydrogen bonds. Hydrophobic attraction stabilizes the structure formed by these forces (Chothia and Janin, 1975). The first vestige of such stereospecific interactions may appear in the low-force $A·M·ADP·P_i$ complex. This complex has a slow dissociation constant (Iwamoto, 1995a) and contributes to fiber stiffness (Brozovich et al., 1988; Iwamoto, 1995a) but shows a high rate of stress relaxation (Iwamoto, 1995a), implying that the stereospecific interactions are not yet intensive.

The stereospecific interactions are likely to be strengthened as the actomyosin reaction proceeds toward the end of the cycle and contractile force is generated (see Highsmith and Murphy, 1992). At one stage in this flow of events, there is an ionic process, i.e., the transition between the two $A·M·ADP$ substates, as we postulated. Because of its IS sensitivity exhibited at the high IS range, it is expected that some salt-bridge formation is involved in this process, and this structure is to some extent still accessible to solvent. Unlike the long-range electrostatic attraction, higher salt concentrations would be needed to disrupt salt bridges (e.g., thick filament backbone, which is stabilized by complementary pairs of charged amino acid residues; McLachlan and Karn, 1982). Such salt bridges may be formed at the second actin-myosin binding sites (Rayment et al., 1993a). Alternatively, salt bridges may be formed within the myosin head. Although intramolecular salt bridges are relatively rare (Schulz and Schirmer, 1979), a number of salt bridges have been reported for the crystal structure of myosin heads from different sources (Rayment et al., 1993b; Fisher et al., 1995; Dominguez et al., 1998). In particular, those formed between the "converter" and "relay loop" regions (Dominguez et al., 1998) may constitute a part of the power stroke.

The last stage of the actomyosin reaction is the formation of the rigor complex, which is very resistant to high IS (Fig. 7). The rigor complex may involve extensive stereospecific interactions stabilized by hydrophobic forces, a configuration similar to other tightly associated oligomeric proteins, such as $\alpha\beta$-oxyhemoglobin dimers (Chothia and Janin, 1975). This dimer is stable in up to 1 M NaCl (Gryczynski et al., 1997).

REFERENCES

Andrews, M. A. W., D. W. Maughan, T. M. Nosek, and R. E. Godt. 1991. Ion-specific and general ionic effects on contraction of skinned fast-twitch skeletal muscle from the rabbit. *J. Gen. Physiol.* 98:1105–1125.

Baker, J. E., I. Brust-Mascher, S. Ramachandran, L. E. LaConte, and D. D. Thomas. 1998. A large and distinct rotation of the myosin light chain domain occurs upon muscle contraction. *Proc. Natl. Acad. Sci. USA.* 95:2944–2949.

Brenner, B. 1987. Mechanical and structural approaches to correlation of cross-bridge action in muscle with actomyosin ATPase in solution. *Annu. Rev. Physiol.* 49:655–672.

Brenner, B., L. C. Yu, and J. M. Chalovich. 1991. Parallel inhibition of active force and relaxed fiber stiffness in skeletal muscle by caldesmon: implications for the pathway to force generation. *Proc. Natl. Acad. Sci. USA.* 88:5739–5743.

Brozovich, F. V., L. D. Yates, and A. M. Gordon. 1988. Muscle force and stiffness during activation and relaxation. Implications for the actomyosin ATPase. *J. Gen. Physiol.* 91:399–420.

Cantor, C. R., and P. R. Schimmel. 1980. Biophysical Chemistry. Part III. The Behavior of Biological Macromolecules. Freeman, New York.

Chothia, C., and J. Janin. 1975. Principles of protein-protein recognition. *Nature.* 256:705–708.

Dantzig, J. A., Y. E. Goldman, N. C. Millar, J. Lacktis, and E. Homsher. 1992. Reversal of the cross-bridge force-generating transition by photogeneration of phosphate in rabbit psoas muscle fibres. *J. Physiol. (Lond.).* 451:247–278.

Dantzig, J. A., M. G. Hibberd, D. R. Trentham, and Y. E. Goldman. 1991. Cross-bridge kinetics in the presence of MgADP investigated by photolysis of caged ATP in rabbit psoas muscle fibres. *J. Physiol. (Lond.).* 432:639–680.

DasGupta, G., and E. Reisler. 1989. Antibody against the amino terminus of alpha-actin inhibits actomyosin interactions in the presence of ATP. *J. Mol. Biol.* 207:833–836.

Davis, J. S. 1999. The Huxley-Simmons phase 2 and force generation. A comparative study. *Biophys. J.* 76:A269.

Dobbie, I., M. Linari, G. Piazzesi, M. Reconditi, N. Koubassova, M. A. Ferenczi, V. Lombardi, and M. Irving. 1998. Elastic bending and active tilting of myosin heads during muscle contraction. *Nature.* 396:383–387.

Dominguez, R., Y. Freyzon, K. M. Trybus, and C. Cohen. 1998. Crystal structure of a vertebrate smooth muscle myosin motor domain and its complex with the essential light chain: visualization of the pre-power stroke state. *Cell.* 94:559–571.

Ebus, J. P., G. J. M. Stienen, and G. Elzinga. 1994. Influence of phosphate and pH on myofibrillar ATPase activity and force in skinned cardiac trabeculae from rat. *J. Physiol. (Lond.).* 476:501–516.

Fisher, A. J., C. A. Smith, J. B. Thoden, R. Smith, K. Sutoh, H. M. Holden, and I. Rayment. 1995. X-ray structures of the myosin motor domain of *Dictyostelium discoideum* complexed with MgADP.BeF$_x$ and MgADP.AlF$_4^-$. *Biochemistry.* 34:8960–8972.

Furch, M., M. A. Geeves, and D. J. Manstein. 1998. Modulation of actin affinity and actomyosin adenosine triphosphatase by charge changes in the myosin motor domain. *Biochemistry.* 37:6317–6326.

Godt, R. E., R. T. H. Fogaca, M. A. W. Andrews, and T. M. Nosek. 1993. Influence of ionic strength on contractile force and energy consumption of skinned fibers from mammalian and crustacean striated muscle. *Adv. Exp. Med. Biol.* 332:763–774.

Goldman, Y. E., and A. F. Huxley. 1994. Actin compliance: are you pulling my chain? *Biophys. J.* 1994:2131–2133.

Gryczynski, Z., S. Beretta, J. Lubokowski, A. Razynska, I. Gryczynski, and E. Bucci. 1997. Time-resolved fluorescence of hemoglobin species. *Biophys. Chem.* 64:81–91.

Gulati, J., and R. J. Podolsky. 1981. Isotonic contraction of skinned muscle fibers on a slow time base. Effects of ionic strength and calcium. *J. Gen. Physiol.* 78:233–257.

Highsmith, S., and A. J. Murphy. 1992. Electrostatic changes at the actomyosin-subfragment 1 interface during force-generating reactions. *Biochemistry.* 31:385–389.

Higuchi, H., T. Yanagida, and Y. E. Goldman. 1995. Compliance of thin filaments in skinned fibers of rabbit skeletal muscle. *Biophys. J.* 69:1000–1010.

Hopkins, S. C., C. Sabido-David, J. E. T. Corrie, M. Irving, and Y. E. Goldman. 1998. Fluorescence polarization transients from rhodamine isomers on the myosin regulatory light chain in skeletal muscle fibers. *Biophys. J.* 74:3093–3110.

Huxley, A. F. 1957. Muscle structure and theories of contraction. *Prog. Biophys. Biophys. Chem.* 7:255–318.

Huxley, A. F., and R. M. Simmons. 1971. Proposed mechanism of force generation in striated muscle. *Nature.* 233:533–538.

Huxley, H. E., M. Kress, A. F. Faruqi, and R. M. Simmons. 1988. X-ray diffraction studies on muscle during rapid shortening and their implications concerning crossbridge behaviour. *Adv. Exp. Med. Biol.* 226:347–352.

Irving, M., T. S. C. Allen, C. Sabido-David, J. S. Craik, B. Brandmeier, J. Kendrick-Jones, J. E. T. Corrie, D. R. Trentham, and Y. E. Goldman. 1995. Tilting of the light-chain region of myosin during step length changes and active force generation in skeletal muscle. *Nature.* 375:688–691.

Israelachvili, J., and R. Pashley. 1982. The hydrophobic interaction is long range, decaying exponentially with distance. *Nature.* 300:341–342.

Iwamoto, H. 1995a. Strain sensitivity and turnover rate of low force cross-bridges in contracting skeletal muscle fibers in the presence of phosphate. *Biophys. J.* 68:243–250.

Iwamoto, H. 1995b. Evidence for increased low force cross-bridge population in shortening skinned skeletal muscle fibers: implications for actomyosin kinetics. *Biophys. J.* 69:1022–1035.

Iwamoto, H. 1998a. Effect of ionic strength on the kinetics of actomyosin interaction in skeletal muscle fibers. *Biophys. J.* 74:A266.

Iwamoto, H. 1998b. Thin filament cooperativity as a major determinant of shortening velocity in skeletal muscle fibers. *Biophys. J.* 74:1452–1464.

Iwamoto, H. 1998c. Effect of a cardiotonic agent, MCI-154, on the contractile properties of skinned skeletal muscle fibers. *Eur. J. Pharmacol.* 341:243–252.

Iwamoto, H., T. Kobayashi, Y. Amemiya, and K. Wakabayashi. 1995. Effect of stretch and release on equatorial x-ray diffraction during a twitch contraction of frog skeletal muscle. *Biophys. J.* 68:227–234.

Julian, F. J., and R. L. Moss. 1981. Effects of calcium and ionic strength on shortening velocity and tension development in frog skinned muscle fibres. *J. Physiol. (Lond.).* 311:179–199.

Kawai, M., K. Güth, K. Winnikes, C. Haist, and J. C. Rüegg. 1987. The effect of inorganic phosphate on the ATP hydrolysis rate and the tension transients in chemically skinned rabbit psoas fibers. *Pflügers Arch.* 408:1–9.

Kawai, M., and H. R. Halvorson. 1991. Two step mechanism of phosphate release and the mechanism of force generation in chemically skinned fibers of rabbit psoas muscle. *Biophys. J.* 59:329–341.

Kawai, M., J. S. Wray, and K. Guth. 1990. Effect of ionic strength on crossbridge kinetics as studied by sinusoidal analysis, ATP hydrolysis rate and X-ray diffraction techniques in chemically skinned rabbit psoas fibres. *J. Muscle Res. Cell Motil.* 11:392–402.

Lehman, W., P. Vibert, P. Uman, and R. Craig. 1995. Steric-blocking by tropomyosin visualized in relaxed vertebrate muscle thin filaments. *J. Mol. Biol.* 251:191–196.

McLachlan, A. D., and J. Karn. 1982. Periodic charge distributions in the myosin rod amino acid sequence match cross-bridge spacings in muscle. *Nature.* 299:226–231.

Mejean, C., M. Boyer, J. P. Labbe, J. Deracourt, Y. Benyamin, and C. Roustan. 1986. Antigenic probes locate the myosin subfragment 1 interaction site on the N-terminal part of actin. *Biosci. Rep.* 6:493–499.

Murphy, K. P., Y. Zhao, and M. Kawai. 1996. Molecular forces involved in force generation during skeletal muscle contraction. *J. Exp. Biol.* 199:2565–2571.

Podolsky, R. J., R. St. Onge, and R. W. Lymn. 1976. X-ray diffraction of actively shortening muscle. *Proc. Natl. Acad. Sci. USA.* 73:813–817.

Rayment, I., H. M. Holden, M. Whittaker, C. B. Yohn, M. Lorenz, K. C. Holmes, and R. A. Milligan. 1993a. Structure of the actin-myosin complex and its implications for muscle contraction. *Science.* 261:58–65.

Rayment, I., W. R. Rypniewski, B. Schmidt-Base, R. Smith, D. R. Tomchick, M. M. Benning, D. A. Winkelmann, G. Wesenberg, and H. M. Holden. 1993b. Three-dimensional structure of myosin subfragment-1: a molecular motor. *Science.* 261:50–58.

Regnier, M., C. Morris, and E. Homsher. 1995. Regulation of the cross-bridge transition from a weakly to strongly bound state in skinned rabbit muscle fibers. *Am. J. Physiol.* 269:C1532–C1539.

Ross, P. D., and S. Subramanian. 1981. Thermodynamics of protein association reactions: forces contributing to stability. *Biochemistry.* 20:3096–3102.

Schulz, G. E., and R. H. Schirmer. 1979. Principles of Protein Structure. Springer-Verlag, Heidelberg.

Seow, C. Y., and L. E. Ford. 1993. High ionic strength and low pH detain activated skinned rabbit skeletal muscle crossbridges in a low force state. *J. Gen. Physiol.*101:487–511.

Somasundaram, B., A. Newport, and R. Tregear. 1989. Slip of rabbit striated muscle in rigor or AMPPNP. *J. Muscle Res. Cell Motil.* 10:360–368.

Sutoh, K., M. Ando, K. Sutoh, and Y. Y. Toyoshima. 1991. Site-directed mutations of *Dictyostelium* actin: disruption of negative charge cluster at the N terminus. *Proc. Natl. Acad. Sci. USA.* 88:7711–7714.

Suzuki, Y., T. Yasunaga, R. Ohkura, T. Wakabayashi, and K. Sutoh. 1998. Swing of the lever arm of a myosin motor at the isomerization and phosphate-release steps. *Nature.* 396:380–383.

Szczesna, D., J. Zhao, and J. D. Potter. 1996. The regulatory light chains of myosin modulate cross-bridge cycling in skeletal muscle. *J. Biol. Chem.* 271:5246–5250.

Wahr, P. A., and J. A. Rall. 1997. Role of calcium and cross bridges in determining rate of force development in frog muscle fibers. *Am. J. Physiol.* 272:C1664–C1671.

Wakabayashi, K., M. Tokunaga, I. Kohno, Y. Sugimoto, T. Hamanaka, Y. Takezawa, T. Wakabayashi, and T. Amemiya. 1992. Small-angle x-ray scattering reveals distinct shape changes of the myosin head during hydrolysis of ATP. *Science.* 258:443–447.

Xiao, M., H. Li, G. E. Snyder, R. Cooke, R. G. Yount, and P. R. Selvin. 1998. Conformational changes between the active-site and regulatory light chain of myosin as determined by luminescence resonance energy transfer: the effect of nucleotides and actin. *Proc. Natl. Acad. Sci. USA.* 95:15309–15314.

Zhao, Y., and M. Kawai. 1994. Kinetic and thermodynamic studies of the cross-bridge cycle in rabbit psoas muscle fibers. *Biophys. J.* 67: 1655–1668.